# Controller Mode and Reference Governor for Constraint and Failure Management in Vehicle Platooning

Ran Tian, Nan Li, Anouck Girard, and Ilya Kolmanovsky

***Abstract*— Vehicle platooning improves traffic efficiency and fuel economy by allowing vehicles to travel together with shorter inter-vehicle distances. Meanwhile, shorter distances also impose increased demand for stricter safety management, including degradation and failure mode effects management. This paper proposes a controller mode and reference governor (CMRG) scheme for constraint and failure management in vehicle platoons. The CMRG is an add-on supervisor for multi-mode controlled systems that monitors and, when necessary, adjusts the control modes and reference inputs to enforce constraints. We show by simulations that with the application of CMRG, safety constraints can be satisfactorily enforced and sensor and/or actuator degradations/failures can be managed in vehicle platoon systems.**

## I. Introduction

A vehicle platoon (see Fig. 1) is a string of vehicles traveling together with a harmonized speed and pre-specified inter-vehicle distances [1]. Vehicle platooning has been shown to be an effective way to improve traffic efficiency and fuel economy [2], [3], and has drawn extensive attention from researchers to address various challenges, including platoon formation [4]–[6], string stability [7]–[9], heterogeneity [10], [11], interaction topology [12], [13] and delay effects [14], [15], etc.

The major benefits of vehicle platooning are attributed to the fact that platooning allows vehicles to travel together with shorter inter-vehicle distances, which can increase road capacity [16] and reduce air resistance for the follower vehicles, thus improving their fuel economy [2]. Since the vehicles are traveling at shorter inter-vehicle distances, safety, in terms of not having collisions, is a major concern.

Many safety requirements, including collision avoidance, can be imposed as constraints during the system operation. Reference governors are add-on, supervisory schemes for closed-loop systems that handle constraints by monitoring, and modifying when necessary, the commands/reference inputs to the system [17].

In this paper, we consider an extension of the reference governor scheme, referred to as the *controller mode and reference governor* (CMRG), which can manipulate both the control modes and reference inputs to the system to enforce constraints, as well as to mitigate degradation/failure effects when they occur. In particular, we apply the CMRG to vehicle platoons to handle safety constraints and sensor and actuator degradations/failures.

The contributions of this paper are as follows: 1) We propose a CMRG scheme for a class of systems with multiple control modes and stochastic disturbance inputs, to probabilistically enforce constraints. 2) We illustrate the use of the proposed CMRG for vehicle platoon constraints and sensor and actuator degradation/failure effects management.

This paper is organized as follows: Section II defines the class of systems to be considered. Section III describes constraints and models to represent sensor and actuator degradations/failures. Section IV presents the CMRG algorithm. In Section V, we introduce in detail the application of CMRG to constraint and failure management in vehicle platooning. Simulation results are reported in Section VI to illustrate the effectiveness of CMRG. Finally, conclusions are given in Section VII.

## II. Multi-Mode Controlled System

In this paper, we consider systems represented by the following discrete-time model,

$$x(k+1) = Ax(k) + B_u u(k) + B_w w(k), \tag{1a}$$

$$y(k) = Cx(k) + D_u u(k) + D_w w(k), \tag{1b}$$

where $x(k) \in \mathbb{R}^{n_x}$ represents the system state at the discrete time instant $k \in \mathbb{Z}_{\geq 0}$, $u(k) \in \mathbb{R}^{n_u}$ represents the control input at time $k$, $w(k) \in \mathbb{R}^{n_w}$ represents a disturbance input at time $k$, and $y(k) \in \mathbb{R}^{n_y}$ represents the system output at time $k$. We assume the disturbance input $w(k)$ takes values randomly and independently based on a normal distribution with mean 0 and covariance $W$, i.e., $w(k) \sim \mathcal{N}(0, W)$ for each $k \in \mathbb{Z}_{\geq 0}$.

We assume that a set of controllers has been defined to stabilize the system to desired steady states. They have the form,

$$u(k) = F^j \hat{x}(k) + G^j v(k), \quad j = 0, 1, ..., n_m, \tag{2}$$

where $\hat{x}(k)$ represents a measurement/estimate of the system state $x(k)$, and $v(k) \in \mathbb{R}^{n_v}$ represents the reference input which determines the desired steady state of the system. In particular, we assume $\hat{x}(k) = x(k) + \tilde{x}(k)$, where $\tilde{x}(k) \sim \mathcal{N}(0, \Sigma_0)$ is a normally-distributed random state measurement/estimate error, independent of $w(k)$. For instance, such an error can be due to the application of a state observer such as a Kalman filter.

This research has been supported by the National Science Foundation Award ECCS 1931738.

Ran Tian, Nan Li, Anouck Girard, and Ilya Kolmanovsky are with the Department of Aerospace Engineering, University of Michigan, Ann Arbor, MI 48109, USA {tianran, nanli, ilya, anouck}@umich.edu.

Substituting (2) into (1), we obtain

$$x(k+1) = \bar{A}^j x(k) + \bar{B}^j v(k) + w_x^j(k), \tag{3a}$$
$$y(k) = \bar{C}^j x(k) + \bar{D}^j v(k) + w_y^j(k), \tag{3b}$$

where $\bar{A}^j = A + B_u F^j$, $\bar{B}^j = B_u G^j$, $\bar{C}^j = C + D_u F^j$, $\bar{D}^j = D_u G^j$, and $w_x^j \sim \mathcal{N}(0, W_x^j)$, $w_y^j \sim \mathcal{N}(0, W_y^j)$, in which $W_x^j = B_u F^j \Sigma_0 (B_u F^j)^\top + B_w W B_w^\top$ and $W_y^j = D_u F^j \Sigma_0 (D_u F^j)^\top + D_w W D_w^\top$.

The variable $j = 0, 1, ..., n_m$ in (2) identifies the *control mode* of the system, which can be selected to handle constraints as well as sensor and actuator degradations. The pairs $(F^j, G^j)$ are assumed to be designed such that 1) the closed-loop dynamics (3a) are stable, and 2) the steady-state output corresponding to $v(k)$ is same for every $j = 0, 1, ..., n_m$. Specifically, this means $\bar{C}^j (I_{n_x} - \bar{A}^j)^{-1} \bar{B}^j + \bar{D}^j$ are identical for all $j$.

## III. Constraints and Failures

### A. Constraints

Constraints may be imposed on system states/outputs to represent safety requirements such as collision avoidance, or be imposed on control inputs to represent, for instance, actuator capability limits. In this paper, we consider constraints that can be written as

$$y(k) \in \mathcal{Y} = \big\{ y \in \mathbb{R}^{n_y} : y \le y_{\text{limit}} \big\}. \tag{4}$$

Note that (4) can represent both state/output and input constraints by properly choosing the matrix pair $(C, D_u)$. For a system modeled as (1) with stochastic inputs, it is typical [18], [19] to enforce the constraint (4) probabilistically as follows:

$$\mathbb{P}\big(y(k) \in \mathcal{Y}\big) \ge \gamma. \tag{5}$$

This is because: On the one hand, it is in general not possible to enforce (4) deterministically due to the presence of the Gaussian uncertainties $w(k) \sim \mathcal{N}(0, W)$ and $\tilde{x}(k) \sim \mathcal{N}(0, \Sigma_0)$, which can take arbitrarily large values with positive probabilities. On the other hand, the parameter $\gamma \in (0, 1)$, representing a probabilistic guarantee for constraint enforcement, can be used as a tuning parameter to balance the tradeoff between performance and robustness, reducing the conservatism of the design.

### B. Degradations and failures

In addition to constraints, the management of degradations and failures is another important task, especially for safety critical systems. Two typical types of failures for control systems are sensor failures and actuator failures.

In this paper, we model a sensor degradation/failure as a change in the measurement covariance $\Sigma_0$. In particular, we consider

$$\tilde{x}(k) \sim \mathcal{N}(0, \Sigma_0^p), \tag{6}$$

where the set of positive semi-definite matrices $\Sigma_0^p$, $p = 0, ..., n_p$, represents the measurement covariance for normal case ($p = 0$) and for pre-specified different degradation/failure cases ($p = 1, ..., n_p$). We remark that modeling sensor failure as a change of $\Sigma_0$ is reasonable as in many safety critical applications, the state measurement $\hat{x}(k)$ used in the control law (2) is obtained by fusing the measurements of multiple, and at times redundant, sensors to reduce the measurement covariance. Then, a failure in one or more of the sensors typically results in an increase in the measurement covariance.

On the other hand, a degradation/failure in an actuator typically causes its capability in terms of providing force or power to decrease, or in other words, causes its capability limits to change. On the basis of the fact that input constraints representing such limits can be incorporated in (4), we model an actuator degradation/failure by considering

$$y(k) \in \mathcal{Y}^q = \big\{ y \in \mathbb{R}^{n_y} : y \le y_{\text{limit}}^q \big\}, \tag{7}$$

where the set of output limits $y_{\text{limit}}^q$, $q = 0, ..., n_q$, represents the constraints (including the actuator limits) for normal case ($q = 0$) and for pre-specified different failure cases ($q = 1, ..., n_q$).

Furthermore, we note that failures in many other subsystems are often handled by limited operating strategy, which restricts the actuator authority (e.g., limp home throttle position, transmission locked in third gear, etc). Such failures can also be represented by changing control input constraints.

## IV. Controller Mode and Reference Governor

The controller mode and reference governor (CMRG) is a supervisor that manages the control mode $j = 0, 1, ..., n_m$ and the reference input $v(k) \in \mathbb{R}^{n_v}$ corresponding to the current status of the system (normal or failure) to enforce constraints. Its operation is based on a collection of output admissible sets defined as follows:

$$\begin{aligned}\mathcal{O}_N(j,p,q) = \big\{ (x_0, v) :\ &\text{If } x(0) \sim \mathcal{N}(x_0, \Sigma_0^p), v(k) \equiv v, \\ &\text{then } \mathbb{P}\big(y^j(k) \in \mathcal{Y}^q\big) \ge \gamma \text{ for } k = 0, 1, ..., N \big\},\end{aligned} \tag{8}$$

where $y^j(k)$ is the output of the system (3) corresponding to the control mode $j$, and $N \in \mathbb{N} \cup \{\infty\}$ is a specified planning horizon. Due to the fact that the construction of $\mathcal{O}_N(j,p,q)$ requires evaluation of $\mathbb{P}\big(y^j(k) \in \mathcal{Y}^q\big)$, which involves integration of the density function of a random vector over a polyhedral set and is in general computationally difficult [20], we consider the following subset of $\mathcal{O}_N(j,p,q)$,

$$\begin{aligned}\tilde{\mathcal{O}}_N(j,p,q) = \big\{ (x_0, v) :\ &\text{If } \hat{x}(0) = x_0, v(k) \equiv v, \\ &\text{then } \hat{y}^j(k) \in \mathcal{Y}^q \sim \mathcal{P}^{j,p}(k) \text{ for } k = 0, 1, ..., N \big\},\end{aligned} \tag{9}$$

where $\hat{y}^j(k)$ is the output of the following disturbance-free system

$$\begin{aligned}\hat{x}(k+1) &= \bar{A}^j \hat{x}(k) + \bar{B}^j v(k), \\ \hat{y}(k) &= \bar{C}^j \hat{x}(k) + \bar{D}^j v(k),\end{aligned} \tag{10}$$

and $\mathcal{Y}^q \sim \mathcal{P}^{j,p}(k) = \big\{ y : y + \tilde{y} \in \mathcal{Y}^q \text{ for all } \tilde{y} \in \mathcal{P}^{j,p}(k) \big\}$ is the P(ontryagin)-difference of the sets $\mathcal{Y}^q$ and $\mathcal{P}^{j,p}(k)$, with $\mathcal{P}^{j,p}(k) = \big\{ y : y^\top (\Upsilon^{j,p}(k))^{-1} y \le F^{-1}(\gamma, n_y) \big\}$ being the

$\gamma$-level confidence ellipsoid, in which $\Upsilon^{j,p}(k)$ is the output of the following system

$$\begin{aligned}\Xi(k+1) &= \bar{A}^j\,\Xi(k)\,(\bar{A}^j)^\top + B_u F^j \Sigma_0^p (B_u F^j)^\top + B_w W B_w^\top,\\ \Upsilon(k) &= \bar{C}^j\,\Xi(k)\,(\bar{C}^j)^\top + D_u F^j \Sigma_0^p (D_u F^j)^\top + D_w W D_w^\top,\end{aligned} \tag{11}$$

with the initial condition $\Xi(0) = \Xi_0^p$, and $F^{-1}(\gamma, n_y)$ is the inverse of the cumulative distribution function of the $\chi^2$ distribution with $n_y$ degrees of freedom evaluated at $\gamma$.

We remark that for the polyhedral set $\mathcal{Y}^q$ defined in (7), $\mathcal{Y}^q \sim \mathcal{P}^{j,p}(k)$ can be computed as [21]

$$\mathcal{Y}^q \sim \mathcal{P}^{j,p}(k) = \tag{12}$$
$$\Big\{y : y_i \le \big(y^q_{\text{limit}}\big)_i - \sqrt{F^{-1}(\gamma, n_y)\big(\Upsilon^{j,p}(k)\big)_{ii}},\ i = 1, ..., n_y\Big\}.$$

Based on (10)-(12), it is easy to see that the set $\tilde{\mathcal{O}}_N(j, p, q)$ is characterized by a set of linear inequalities acting on the pair $(x_0, v)$. The numerical procedure to construct $\tilde{\mathcal{O}}_N(j, p, q)$ is similar to Section 3.2 of [19], and is omitted here.

The CMRG operates based on the following Algorithm 1. In Algorithm 1, $\hat{v}(k)$ denotes the original reference input at time $k$, which may represent the maneuver command from a human operator or be generated by a higher-level planning algorithm without accounting for constraints or failures, and $\|\cdot\|_S = \sqrt{(\cdot)^\top S(\cdot)}$ with $S$ being a positive definite matrix. After the control mode and reference pair $(j(k), v(k))$ is determined by CMRG, the system is switched to the mode $j = j(k)$ for one step with the reference input $v(k)$.

**Algorithm 1:** CMRG Operation

**Input** Current sensor and actuator status $\big(p(k), q(k)\big)$ and state measurement $\hat{x}(k)$.
**Output** Current control mode $j(k)$ and reference $v(k)$.
**Function** $\big(j(k), v(k)\big) = \textbf{CMRG}\big(p(k), q(k), \hat{x}(k)\big)$
Solve: $\min_{v^0} \|v^0 - \hat{v}(k)\|_S^2$ subject to $(\hat{x}(k), v^0) \in \tilde{\mathcal{O}}_N\big(0, p(k), q(k)\big)$;
**if** *solution exists* **then**
  **return** $(0, v^0)$.
**else**
  $V \leftarrow \emptyset$;
  **for** $j = 1, 2, ..., n_m$ **do**
    Solve: $\min_{v^j} \|v^j - \hat{v}(k)\|_S^2$ subject to $(\hat{x}(k), v^j) \in \tilde{\mathcal{O}}_N\big(j, p(k), q(k)\big)$;
    If solution exists, then $V \leftarrow V \cup \{v^j\}$;
  **end for**
  Find $v^{j^*} = \arg\min_{v^j \in V} \|v^j - \hat{v}(k)\|_S^2$ and **return** $(j^*, v^{j^*})$.
**end if**

When CMRG cannot find a feasible pair $(j(k), v(k))$ after searching over all available control modes $j = 0, 1, ..., n_m$ (which may result from the occurrence of a very large disturbance input realization), as a fail-safe, CMRG relaxes the constraint $y^q_{\text{limit}}$ to $y^q_{\text{limit}} + \lambda$ with $\lambda \ge 0$ as an optimization variable representing the degree of constraint violation. Correspondingly, the constraint $(\hat{x}(k), v^j) \in \tilde{\mathcal{O}}_N\big(j, p(k), q(k)\big)$ is relaxed by replacing each of the inequality (12) with

$$y_i \le \big(y^q_{\text{limit}}\big)_i + \lambda - \sqrt{F^{-1}(\gamma, n_y)\big(\Upsilon^{j,p}(k)\big)_{ii}}. \tag{13}$$

After that, CMRG solves for the pair $(j^*, v^{j^*})$ with the minimum violation $\lambda$.

Theoretical properties of the CMRG defined by Algorithm 1, including probabilistic constraint enforcement and convergence of $v(k)$ to constant $\hat{v}(k)$, can be characterized following similar steps as in the *stochastic reference governor* in [19]. Rigorous statements and proofs of these properties will be pursued in our future work.

## V. Constraint and Failure Management in Vehicle Platooning

We apply the proposed controller mode and reference governor (CMRG) scheme to constraint and failure management in vehicle platooning (illustrated in Fig. 1). We first introduce the models to represent the longitudinal dynamics of a vehicle platoon and the control law to realize car-following behavior. We then introduce the models that represent constraints and sensor/actuator failures. After that, we discuss the incorporation of these models into the CMRG scheme to achieve constraint and failure management.

### A. Car-following dynamics and control

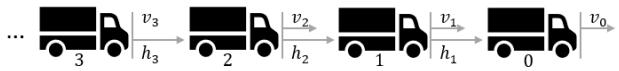


Fig. 1. Vehicle platooning illustration.

In a vehicle platoon, each vehicle $i = 1, ..., n_v$ follows its preceding vehicle $i-1$ according to the following dynamics

$$\dot{h}_i(t) = v_{i-1}(t) - v_i(t), \tag{14a}$$
$$\dot{v}_i(t) = u_i(t), \tag{14b}$$

where $h_i$ denotes vehicle $i$'s headway distance to vehicle $i-1$, $v_i$ denotes vehicle $i$'s longitudinal speed, and $u_i$ denotes its longitudinal acceleration and is the controlled signal.

In particular, we consider the following controller for $u_i$,

$$u_i(t) = \hat{u}_i(k\Delta t), \tag{15}$$

for $t \in [k\Delta t, (k+1)\Delta t)$, where

$$\hat{u}_i(t) = \alpha_i\big(\hat{h}_i(t) - h_i^r(t)\big) + \beta_i\big(\hat{v}_{i-1}(t) - v_i(t)\big), \tag{16}$$

in which $\hat{h}_i$ is a measurement of the headway distance $h_i$, $\hat{v}_{i-1}$ is a measurement of the preceding vehicle's speed $v_{i-1}$, the gain $\alpha_i$ is to match the measured headway distance $\hat{h}_i$ to a reference headway distance $h_i^r$, and the gain $\beta_i$ is to match the ego vehicle's speed $v_i$ to the measured speed of the preceding vehicle $\hat{v}_{i-1}$. In particular, we assume $\hat{h}_i(t) = h_i(t) + \tilde{h}_i(t)$ and $\hat{v}_{i-1}(t) = v_{i-1}(t) + \tilde{v}_{i-1}(t)$, where $\tilde{h}_i(t) \sim \mathcal{N}(0, w_i^h)$ and $\tilde{v}_{i-1}(t) \sim \mathcal{N}(0, w_i^v)$ are normally distributed

random measurement errors. Note that the piecewise constant control signal (15) accounts for the fact that measurements are taken at sample time instants $t = k\Delta t$, $k \in \mathbb{Z}_{\geq 0}$. Note also that we assume each vehicle $i$ can measure its own speed $v_i(t)$ perfectly.

Substituting (15) and (16) into (14), we obtain

$$\dot{h}_i(t) = v_{i-1}(t) - v_i(t), \tag{17a}$$

$$\dot{v}_i(t) = \alpha_i\big(h_i(k\Delta t) - h_i^r(k\Delta t)\big) + \beta_i\big(v_{i-1}(k\Delta t) - v_i(k\Delta t)\big) + \alpha_i\tilde{h}_i(k\Delta t) + \beta_i\tilde{v}_{i-1}(k\Delta t), \tag{17b}$$

for $t \in [k\Delta t, (k+1)\Delta t)$, $k \in \mathbb{Z}_{\geq 0}$.

Assuming $v_{i-1}(t)$ stays constant over $[k\Delta t, (k+1)\Delta t)$ and integrating (17), we further obtain

$$h_i(k+1) = \big(1 - \frac{\Delta t^2}{2}\alpha_i\big)h_i(k) - \big(\Delta t - \frac{\Delta t^2}{2}\beta_i\big)v_i(k) + \frac{\Delta t^2}{2}\alpha_i h_i^r(k) + \big(\Delta t - \frac{\Delta t^2}{2}\beta_i\big)v_{i-1}(k) - \frac{\Delta t^2}{2}\big(\alpha_i\tilde{h}_i(k) + \beta_i\tilde{v}_{i-1}(k)\big), \tag{18a}$$

$$v_i(k+1) = \Delta t\,\alpha_i h_i(k) + (1 - \Delta t\,\beta_i)v_i(k) - \Delta t\,\alpha_i h_i^r(k) + \Delta t\,\beta_i v_{i-1}(k) + \Delta t\big(\alpha_i\tilde{h}_i(k) + \beta_i\tilde{v}_{i-1}(k)\big). \tag{18b}$$

Note that the $k$ and $k+1$ in the above expressions denote the discrete-time instants $k\Delta t$ and $(k+1)\Delta t$.

In matrix form, the discrete-time dynamics (18) can be written as

$$x_i(k+1) = A_i x_i(k) + B_i h_i^r(k) + \Phi_i v_{i-1}(k) + \Psi_i w_i(k), \tag{19}$$

where $x_i(k) = \big[h_i(k),\, v_i(k)\big]^\top$, $w_i(k) = \big[\tilde{h}_i(k),\, \tilde{v}_{i-1}(k)\big]^\top$ and

$$A_i = \begin{bmatrix} 1 - \frac{\Delta t^2}{2}\alpha_i & -\Delta t + \frac{\Delta t^2}{2}\beta_i \\ \Delta t\,\alpha_i & 1 - \Delta t\,\beta_i \end{bmatrix}, \quad B_i = \begin{bmatrix} \frac{\Delta t^2}{2}\alpha_i \\ -\Delta t\,\alpha_i \end{bmatrix},$$
$$\Phi_i = \begin{bmatrix} \Delta t - \frac{\Delta t^2}{2}\beta_i \\ \Delta t\,\beta_i \end{bmatrix}, \quad \Psi_i = \begin{bmatrix} -\frac{\Delta t^2}{2}\alpha_i & -\frac{\Delta t^2}{2}\beta_i \\ \Delta t\,\alpha_i & \Delta t\,\beta_i \end{bmatrix}. \tag{20}$$

In principle, the reference headway distance $h_i^r$, which determines the steady-state car-following distance as $h_i^* = h_i^r$, is a design variable. Oftentimes, it is designed as a function, called a *range policy*, of the ego vehicle's steady-state speed, which is determined by the preceding vehicle's speed $v_{i-1}$, i.e., $h_i^r(k) = G\big(v_{i-1}(k)\big)$. In this paper, we consider the following range policy, which is modified from the range policies proposed in [11], [22],

$$h_i^r(k) = G\big(v_{i-1}(k)\big) = \begin{cases} h_{\text{lo}} & 0 \leq v_{i-1}(k) \leq v_{\text{lo}}, \\ h_{\text{lo}} + \frac{v_{i-1}(k) - v_{\text{lo}}}{v_{\text{up}} - v_{\text{lo}}}(h_{\text{up}} - h_{\text{lo}}) & v_{\text{lo}} \leq v_{i-1}(k) \leq v_{\text{up}}, \\ h_{\text{up}} & v_{i-1}(k) \geq v_{\text{up}}. \end{cases} \tag{21}$$

### B. Car-following constraints

Two types of constraints are considered in this paper. The first type is imposed on the headway distance $h_i(k)$. On the one hand, $h_i(k)$ should not be too small to avoid front-end collisions; on the other hand, $h_i(k)$ should not be too large to prevent other cars from cutting in. Specifically, we consider the following constraints on $h_i(k)$,

$$h_{\min} \leq h_i(k) \leq h_{\max}. \tag{22}$$

The second type of constraints represents actuator capability limits. In particular, we consider the following constraints on $u_i(k)$,

$$a_{\min} \leq u_i(k) = \alpha_i\big(h_i(k) + \tilde{h}_i(k) - h_i^r(k)\big) + \beta_i\big(v_{i-1}(k) + \tilde{v}_{i-1}(k) - v_i(k)\big) \leq a_{\max}. \tag{23}$$

For instance, the upper bound $a_{\max} > 0$ may represent an engine power limit and the lower bound $a_{\min} < 0$ may represent a braking force limit.

In matrix form, the constraints (22) and (23) can be written as

$$\begin{bmatrix} h_{\min} \\ a_{\min} \end{bmatrix} \leq y_i(k) \leq \begin{bmatrix} h_{\max} \\ a_{\max} \end{bmatrix}, \tag{24}$$

where

$$y_i(k) = C_i x_i(k) + D_i h_i^r(k) + \Theta_i v_{i-1}(k) + \Xi_i w_i(k), \tag{25}$$

$$C_i = \begin{bmatrix} 1 & 0 \\ \alpha_i & -\beta_i \end{bmatrix}, \quad D_i = \begin{bmatrix} 0 \\ -\alpha_i \end{bmatrix}, \tag{26}$$

$$\Theta_i = \begin{bmatrix} 0 \\ \beta_i \end{bmatrix}, \quad \Xi_i = \begin{bmatrix} 0 & 0 \\ \alpha_i & \beta_i \end{bmatrix}. \tag{27}$$

As has been discussed in Section III-A, due to the fact that the disturbance input $w_i(k) = \big[\tilde{h}_i(k),\, \tilde{v}_{i-1}(k)\big]^\top$ is modeled as a Gaussian noise and has a positive probability to take arbitrarily large values, in general, the constraint (24) cannot be enforced deterministically. Instead, we consider a probabilistic counterpart of (24) as follows,

$$\mathbb{P}\left( \begin{bmatrix} h_{\min} \\ a_{\min} \end{bmatrix} \leq y_i(k) \leq \begin{bmatrix} h_{\max} \\ a_{\max} \end{bmatrix} \right) \geq \gamma, \tag{28}$$

with $\gamma \in (0, 1)$.

### C. Sensor and actuator failures

*1) Sensor failure:* The $\hat{h}_i$ and $\hat{v}_{i-1}$ values used to compute the control (16) are usually derived by fusing the measurements of multiple sensors, such as radar, lidar and camera, so that uncertainty can be reduced. In turn, a failure in one or more of the sensors typically results in an increase in the uncertainty. Therefore, we model a sensor failure as a change in the measurement covariance. In particular,

$$w_i(k) = \big[\tilde{h}_i(k) \quad \tilde{v}_{i-1}(k)\big]^\top \sim \mathcal{N}(0, W_i^p), \tag{29}$$

where $W_i^p$ is a positive semi-definite covariance matrix for each $p$, with $p = 0$ corresponding to the normal measurement covariance and $p = 1, ..., n_p$ corresponding to the covariances at a pre-specified set of sensor failure cases. For instance, suppose $\hat{h}_i$ and $\hat{v}_{i-1}$ are derived by fusing the radar, lidar and camera measurements. Then, depending on the state of health of each of the three sensors, there are in total 8 cases, including 1 normal case, and $n_p = 7$ failure cases.

*2) Actuator failure:* As introduced in Section V-B, the bounds $a_{\max}$ and $a_{\min}$ on $u_i$ represent engine/braking system capability limits. We model a degradation/failure in these systems as a change in the values of these bounds. In particular,

$$a^q_{\min} \leq u_i(k) \leq a^q_{\max}, \tag{30}$$

with $q = 0$ corresponding to the normal actuator limits and $q = 1, ..., n_q$ corresponding to the limits at a pre-specified set of actuator failure cases.

### D. Constraint and failure management using CMRG

As a predictive scheme, CMRG manages constraints relying on a prediction of the system operating condition over a horizon.

Let $k = 0$ denote the current sample time instant and assume that a measurement $\hat{v}_{i-1}(0)$ of the preceding vehicle's current speed $v_{i-1}(0)$ has been obtained. We model the variations in preceding vehicle's speed over the horizon stochastically as follows:

$$v_{i-1}(k) = v_{i-1}(0) + \tilde{\bar{v}}_{i-1}(k), \tag{31}$$

where $\tilde{\bar{v}}_{i-1}(k) \sim \mathcal{N}(0, w^{\text{pre}}_{i-1})$.

Then, after augmenting the trivial dynamics $v_{i-1}(0) = v_{i-1}(0)$ to the model (19), (25) and incorporating multiple designs for the gains $(\alpha, \beta)$ in the control law (16) as well as possible adjustments of the reference signal $h^r_i(k)$, we obtain the following predictive model

$$\bar{x}_i(k+1) = \bar{A}^j_i \bar{x}_i(k) + \bar{B}^j_i \mu + \bar{\Psi}^j_i \bar{w}_i(k), \tag{32a}$$

$$y(k) = \bar{C}^j_i \bar{x}_i(k) + \bar{D}^j_i \mu + \bar{\Xi}^j_i \bar{w}_i(k), \tag{32b}$$

where $\bar{x}_i(k) = \left[h_i(k),\, v_{i-1}(0),\, v_i(k)\right]^\top$, $\bar{w}_i(k) = \left[\tilde{h}_i(k),\, \tilde{v}_{i-1}(k),\, \tilde{\bar{v}}_{i-1}(k)\right]^\top$, and

$$\bar{A}^j_i = \begin{bmatrix} 1 - \frac{\Delta t^2}{2}\alpha^j_i & \Delta t - \frac{\Delta t^2}{2}\beta^j_i & -\Delta t + \frac{\Delta t^2}{2}\beta^j_i \\ 0 & 1 & 0 \\ \Delta t\, \alpha^j_i & \Delta t\, \beta^j_i & 1 - \Delta t\, \beta^j_i \end{bmatrix}, \tag{33}$$

$$\bar{B}^j_i = \begin{bmatrix} \frac{\Delta t^2}{2}\alpha^j_i \\ 0 \\ -\Delta t\, \alpha^j_i \end{bmatrix}, \bar{\Psi}^j_i = \begin{bmatrix} -\frac{\Delta t^2}{2}\alpha^j_i & -\frac{\Delta t^2}{2}\beta^j_i & \Delta t - \frac{\Delta t^2}{2}\beta^j_i \\ 0 & 0 & 0 \\ \Delta t\, \alpha^j_i & \Delta t\, \beta^j_i & \Delta t\, \beta^j_i \end{bmatrix},$$

$$\bar{C}^j_i = \begin{bmatrix} 1 & 0 & 0 \\ \alpha^j_i & \beta^j_i & -\beta^j_i \end{bmatrix}, \bar{D}^j_i = \begin{bmatrix} 0 \\ -\alpha^j_i \end{bmatrix}, \bar{\Xi}^j_i = \begin{bmatrix} 0 & 0 & 0 \\ \alpha^j_i & \beta^j_i & \beta^j_i \end{bmatrix}.$$

The first two components of the initial condition $\bar{x}_i(0) = \left[h_i(0),\, v_{i-1}(0),\, v_i(0)\right]^\top$ are not perfectly measured but can be estimated using the measurements $\hat{h}_i(0)$ and $\hat{v}_{i-1}(0)$ based on

$$\bar{x}_i(0) \sim \mathcal{N}\left( \begin{bmatrix} \hat{h}_i(0) \\ \hat{v}_{i-1}(0) \\ v_i(0) \end{bmatrix}, \begin{bmatrix} W^p_i & 0 \\ 0 & 0 \end{bmatrix} \right). \tag{34}$$

The disturbance input $\bar{w}_i(k) = \left[\tilde{h}_i(k),\, \tilde{v}_{i-1}(k),\, \tilde{\bar{v}}_{i-1}(k)\right]^\top$ takes values based on

$$\bar{w}_i(k) \sim \mathcal{N}\left(0, \begin{bmatrix} W^p_i & 0 \\ 0 & w^{\text{pre}}_{i-1} \end{bmatrix}\right). \tag{35}$$

Furthermore, we have replaced the reference headway distance $h^r_i(k)$ in the model (19) with $\mu$ in (32), which is determined by solving the following optimization problem

$$\min_{\mu} \left(\mu - G(\hat{v}_{i-1}(0))\right)^2, \tag{36}$$

where $G(\cdot)$ is the range policy (21), subject to the model (32) and the following probabilistic constraint for $k = 0, 1, ..., N$,

$$\mathbb{P}\left( \begin{bmatrix} h_{\min} \\ a^q_{\min} \end{bmatrix} \leq y_i(k) \leq \begin{bmatrix} h_{\max} \\ a^q_{\max} \end{bmatrix} \right) \geq \gamma, \quad \gamma \in (0, 1). \tag{37}$$

Up to this point, we have identified the model (3) in (32), the sensor failure model (6) in (34), (35) with $p = 0, 1, ..., n_p$, and the actuator failure model (7) in (37) with $q = 0, 1, ..., n_q$ for the specific system of vehicle platooning. Then, we can apply the CMRG defined by Algorithm 1 to manage the constraints and failures of this vehicle platooning system.

## VI. Results

In this section, we present simulation results of applying CMRG to constraint and failure management in vehicle platooning.

### A. Model and control parameters

The sampling time $\Delta t$ is chosen as $0.1[s]$. We consider the following set of control gain pairs (i.e., control modes) for (16): $(\alpha^j_i, \beta^j_i) \in \{0.5,\, 1,\, 1.5,\, 2\} \times \{0.5,\, 1,\, 1.5,\, 2,\, 2.5,\, 3\}$, where $(\alpha^0_i, \beta^0_i) = (1, 3)$ is the nominal/default pair. The parameter values for the range policy (21) are $h_{\text{lo}} = 2[m]$, $h_{\text{up}} = 30[m]$, $v_{\text{lo}} = 0[m/s]$, and $v_{\text{up}} = 30[m/s]$. The constraints on the headway distance are set as $h_{\max} = 25[m]$ and $h_{\min} = 16[m]$. The normal measurement covariance is assumed to be $W^{\text{normal}}_i = \text{diag}(0.01^2, 0.02^2)$. The normal acceleration limits are assumed to be $a^{\text{normal}}_{\max} = 3[m/s^2]$ and $a^{\text{normal}}_{\min} = -3[m/s^2]$. For the CMRG design, we set the variance $w^{\text{pre}}_{i-1}$ that accounts for the variations in the preceding vehicle's speed $v_{i-1}(k)$ over the planning horizon as $w^{\text{pre}}_{i-1} = 0.2^2$. The probabilistic constraint satisfaction parameter $\gamma$ is chosen to be $0.99$.

### B. Sensor failure management in a two-vehicle platoon

The first example that we consider represents the scenario where a sensor failure occurs to the follower vehicle in a two-vehicle platoon. It is assumed that the leader vehicle (indexed by 0) drives with a trapezoidal speed profile $v_0$, which corresponds to the reference headway distance profile $h^r_1$ shown by the blue dash-dotted curve in Fig. 2(a) according to the range policy $h^r_1 = G(\hat{v}_0)$ in (21). We assume that at the time instant $t_f = 12.5[s]$, a failure occurs to the follower vehicle's sensor system, which increases the measurement covariance from $W^{\text{normal}}_1 = \text{diag}(0.01^2, 0.02^2)$ to $W^{\text{degraded}}_1 = \text{diag}(0.04^2, 0.08^2)$.

In Fig. 2, we plot the reference $\mu$, headway distance $h_1$ and acceleration $u_1$ profiles of the follower vehicle for the cases when there is no supervision on its controller mode and reference (i.e., $j \equiv 0$ and $\mu \equiv h^r_1$), when a reference governor (RG) [19] is used to supervise its reference $\mu$ but provides no supervision on its controller mode (i.e., $j \equiv 0$),

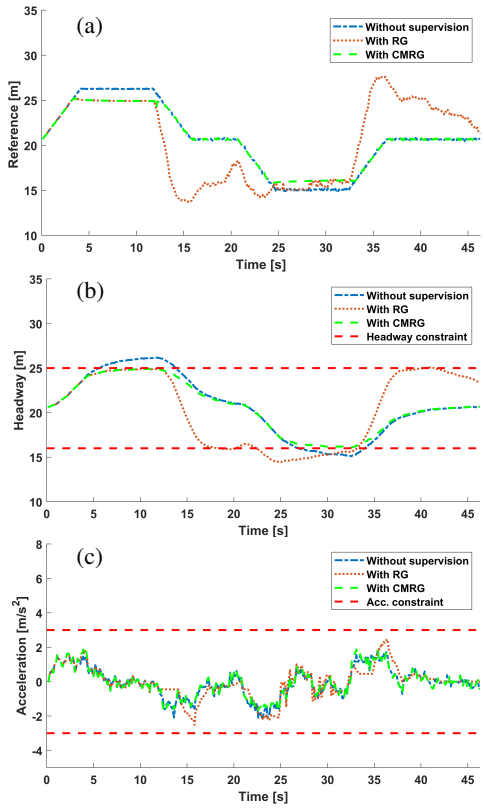


Fig. 2. (a) Original reference (blue), reference governor (RG) output (red), and CMRG output (green) profiles of the follower vehicle. (b) Headway distance profiles of the follower vehicle without supervision on controller mode and reference (blue), with supervision only on the reference using an RG (red), and with CMRG. (c) Acceleration profiles of the follower vehicle without supervision (blue), with RG (red), and with CMRG (green).

and when CMRG is used to supervise both its controller mode and reference. We remark that the RG algorithm is similar to Algorithm 1 for CMRG, but does not search over the ancillary controller modes $j = 1, 2, ..., n_m$ for feasible solutions and switches directly to the fail-safe mode described in the paragraph around (13) after Step 7.

It can be observed that when no supervision is used, the headway distance constraints $h_{\max}$ and $h_{\min}$ are violated. When the reference input $\mu$ is adjusted using an RG, the follower vehicle successfully keeps its headway distance within the constrained range before the sensor failure occurs. However, after the sensor failure occurs, not only a large deviation of $\mu$ from $h_1^r$ is observed but this large deviation also causes the follower vehicle to fail to maintain its headway distance satisfying the lower bound $h_{\min}$. This is because when the sensor failure occurs and the measurement covariance increases, the size of the output admissible set $\tilde{\mathcal{O}}_N$ gets decreased, i.e., fewer state measurement and reference input pairs are constraint admissible. When the control gains $(\alpha, \beta)$ are fixed, to enforce constraints, the RG either has to significantly adjust the reference value or cannot identify a feasible solution. In contrast, when CMRG is used, the follower vehicle successfully maintains constraint satisfaction both before and after the sensor failure. This is attributed to the fact that by issuing the follower vehicle the flexibility of choosing control gain values from a set, the follower vehicle possesses a larger set of feasible state measurement and reference input pairs. The CMRG identifies the optimal pair of controller mode $j$ and reference input $\mu$ in terms of minimizing the deviation of $\mu$ from $h_1^r$.

Fig. 3 plots the profile of the control gain pairs $(\alpha, \beta)$ selected by CMRG. It can be observed that over a short period after the sensor failure occurs at $t_f = 12.5[s]$, CMRG switches the gain $\beta$ from its default value 3 to 2, which facilitates constraint enforcement.

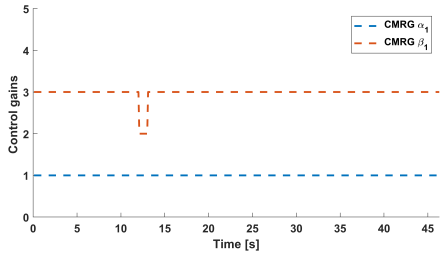


Fig. 3. Control gain profiles of the follower vehicle selected by CMRG.

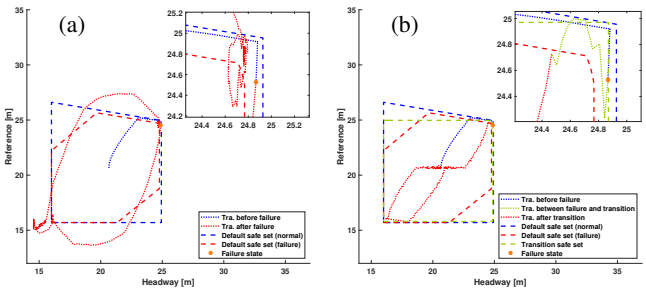


Fig. 4. Projections of output admissible sets and vehicle trajectories on the $(h_1, \mu)$ plane; (a) corresponds to RG supervision; (b) corresponds to CMRG supervision.

In Fig. 4, we plot the projections of the output admissible sets $\tilde{\mathcal{O}}_N$ and trajectories of the follower vehicle on the $(h_1, \mu)$ plane. The blue and red dashed polygons in Fig. 4(a) show the sets $\tilde{\mathcal{O}}_N$ used by RG before and after the sensor failure, respectively, and the dotted curve shows the trajectory under RG supervision (corresponding to the red dotted curves in Fig. 2(a-b)). It can be observed that before the occurrence of sensor failure, the trajectory is maintained within the $\tilde{\mathcal{O}}_N$ set for normal case (the blue dashed polygon). However, when the sensor failure occurs, the immediate state of the follower vehicle (highlighted by the orange point) falls outside of the $\tilde{\mathcal{O}}_N$ set for failure case (the red dashed polygon), which has a reduced size compared to the one for normal case. This causes the failure of the RG in terms of maintaining constraint satisfaction, as shown in Fig. 2.

In contrast, when CMRG is used, it switches the default controller mode to a transition mode when failure occurs (corresponding to the control gain switch shown in Fig. 3).

The $\tilde{\mathcal{O}}_N$ set corresponding to this transition mode (the green dashed polygon in Fig. 4(b)) contains the vehicle state at the failure time, implying the existence of a feasible solution to the reference input $\mu$. Therefore, CMRG satisfactorily maintains constraint satisfaction. After the trajectory enters the $\tilde{\mathcal{O}}_N$ set for failure case corresponding to the default controller mode (the red dashed polygon), CMRG switches the mode back to default.

### C. Sensor and brake failure management in two/three-vehicle platoons

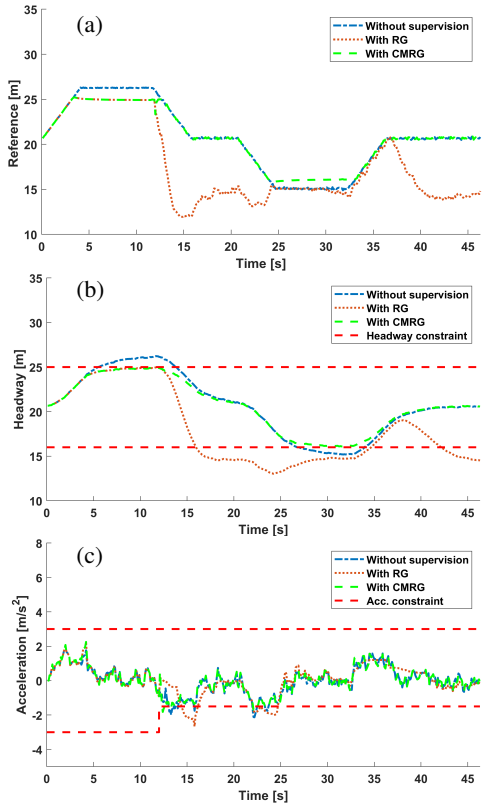


Fig. 5. (a) Original reference (blue), reference governor (RG) output (red), and CMRG output (green) profiles of the follower vehicle. (b) Headway distance profiles of the follower vehicle without supervision on controller mode and reference (blue), with supervision only on the reference using an RG (red), and with CMRG. (c) Acceleration profiles of the follower vehicle without supervision (blue), with RG (red), and with CMRG (green).

We then consider the case where the sensor failure considered in the first example and a failure of the brake system occur concurrently at $t_f = 12.5[s]$ to the follower vehicle (vehicle 1). Although such a simultaneous occurrence of multiple failures may be rare in reality, we consider this extreme case to test the robustness of our CMRG design. In particular, we assume that after the brake failure occurs, the deceleration capability of the vehicle is restricted from $a_{\min}^{\text{normal}} = -3[m/s^2]$ to $a_{\min}^{\text{degraded}} = -1.5[m/s^2]$. Such a change in the lower acceleration limit is also illustrated by the red dashed lines in panel (c) of Figs. 5 and 7.

Similar to Fig. 2, Fig. 5 plots the reference $\mu_1$, headway distance $h_1$ and acceleration $u_1$ profiles of vehicle 1 for without supervision, with RG or CMRG supervisions by blue, red and green curves, respectively. Similar to the results in Fig. 2, when without supervision, the headway distance and acceleration constraints are both violated. The application of RG can maintain the headway distance within the constrained range before failures, but fails to do so after failures occur. Again, this is due to the fact that only adjusting the reference inputs does not grant enough flexibility to handle the failure effects. In contrast, when CMRG is used to supervise both controller mode and reference input selections, the vehicle successfully maintains headway distance constraint satisfaction and violates the acceleration constraint only slightly. Note that such a slight constraint violation is due to the probabilistic enforcement of constraints in (37). Fig. 6 plots the profile of the control gain pairs $(\alpha, \beta)$ selected by CMRG. The CMRG switches the gain pair $(\alpha, \beta)$ from their default values $(1, 3)$ to $(0.5, 1)$ over a short period to compensate the failure effects.

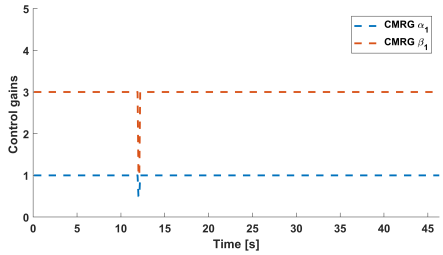


Fig. 6. Control gain profiles of the follower vehicle selected by CMRG.

Lastly, we illustrate the effects of the application of CMRG for constraint and failure management to the entire platoon by plotting the responses of the vehicle (vehicle 2) immediately following the vehicle under sensor and actuator failures (vehicle 1). We assume that both vehicles use CMRG to supervise their controller mode and reference input selections. Note that the speed profile of vehicle 1, $v_1$, determines the original reference headway distance profile for vehicle 2, $h_2^r$, according to the range policy $h_2^r = G(\hat{v}_1)$.

The reference $\mu_1, \mu_2$, headway distance $h_1, h_2$ and acceleration $u_1, u_2$ profiles of vehicles 1 and 2 are shown in Fig. 7. It can be seen that the headway distance constraint for vehicle 2, $h_{\min} \leq h_2 \leq h_{\max}$, is maintained. Note also that the lower acceleration limit for vehicle 2 is $a_{\min}^{\text{normal}} = -3[m/s^2]$ over the entire simulation, since we assume that vehicle 2 does not have a brake failure.

## VII. Conclusion

In this paper, we have considered the application of a controller mode and reference governor (CMRG) scheme to constraint and failure management in vehicle platooning. The CMRG is an add-on supervisor for multi-mode controlled systems that monitors and, when necessary, adjusts the control modes and reference inputs to enforce constraints. Simulation results have been reported to illustrate that with the application of CMRG, safety constraints can be satisfactorily enforced and sensor and/or actuator degradations/failures can be managed in vehicle platoon systems.

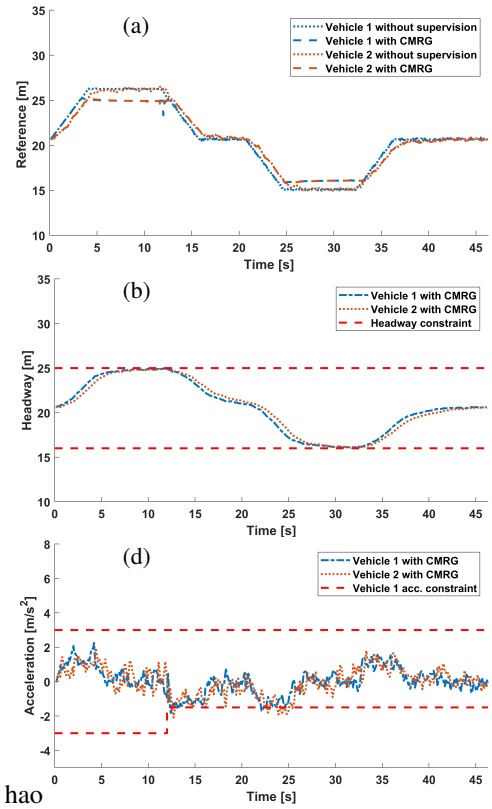


Fig. 7. (a) Original reference and CMRG output profiles of vehicles 1 and 2. (b) Headway distance profiles of vehicles 1 and 2 under CMRG supervisions. (c) Acceleration profiles of vehicles 1 and 2 under CMRG supervisions.

## REFERENCES


[1] S. Maiti, S. Winter, and L. Kulik, "A conceptualization of vehicle platoons and platoon operations," *Transportation Research Part C: Emerging Technologies*, vol. 80, pp. 1–19, 2017.

[2] A. Alam, B. Besselink, V. Turri, J. Martensson, and K. H. Johansson, "Heavy-duty vehicle platooning for sustainable freight transportation: A cooperative method to enhance safety and efficiency," *IEEE Control Systems Magazine*, vol. 35, no. 6, pp. 34–56, 2015.

[3] C. R. He, I. G. Jin, and G. Orosz, "Fuel efficient connected cruise control for heavy-duty trucks in real traffic," *IEEE Transactions on Control Systems Technology*, 2019.

[4] F. Lin, M. Fardad, and M. R. Jovanovic, "Optimal control of vehicular formations with nearest neighbor interactions," *IEEE Transactions on Automatic Control*, vol. 57, no. 9, pp. 2203–2218, 2011.

[5] K.-Y. Liang, J. Mårtensson, and K. H. Johansson, "Heavy-duty vehicle platoon formation for fuel efficiency," *IEEE Transactions on Intelligent Transportation Systems*, vol. 17, no. 4, pp. 1051–1061, 2015.

[6] Y. Li, C. Tang, K. Li, S. Peeta, X. He, and Y. Wang, "Nonlinear finite-time consensus-based connected vehicle platoon control under fixed and switching communication topologies," *Transportation Research Part C: Emerging Technologies*, vol. 93, pp. 525–543, 2018.

[7] P. Seiler, A. Pant, and K. Hedrick, "Disturbance propagation in vehicle strings," *IEEE Transactions on Automatic Control*, vol. 49, no. 10, pp. 1835–1842, 2004.

[8] W. B. Dunbar and D. S. Caveney, "Distributed receding horizon control of vehicle platoons: Stability and string stability," *IEEE Transactions on Automatic Control*, vol. 57, no. 3, pp. 620–633, 2011.

[9] S. S. Avedisov and G. Orosz, "Analysis of connected vehicle networks using network-based perturbation techniques," *Nonlinear Dynamics*, vol. 89, no. 3, pp. 1651–1672, 2017.

[10] F. Gao, S. E. Li, Y. Zheng, and D. Kum, "Robust control of heterogeneous vehicular platoon with uncertain dynamics and communication delay," *IET Intelligent Transport Systems*, vol. 10, no. 7, pp. 503–513, 2016.

[11] N. I. Li and G. Orosz, "Dynamics of heterogeneous connected vehicle systems," *IFAC-PapersOnLine*, vol. 49, no. 10, pp. 171–176, 2016.

[12] Y. Zheng, S. E. Li, J. Wang, D. Cao, and K. Li, "Stability and scalability of homogeneous vehicular platoon: Study on the influence of information flow topologies," *IEEE Transactions on Intelligent Transportation Systems*, vol. 17, no. 1, pp. 14–26, 2015.

[13] L. Zhang and G. Orosz, "Motif-based design for connected vehicle systems in presence of heterogeneous connectivity structures and time delays," *IEEE Transactions on Intelligent Transportation Systems*, vol. 17, no. 6, pp. 1638–1651, 2016.

[14] I. G. Jin and G. Orosz, "Dynamics of connected vehicle systems with delayed acceleration feedback," *Transportation Research Part C: Emerging Technologies*, vol. 46, pp. 46–64, 2014.

[15] W. B. Qin and G. Orosz, "Scalable stability analysis on large connected vehicle systems subject to stochastic communication delays," *Transportation Research Part C: Emerging Technologies*, vol. 83, pp. 39–60, 2017.

[16] Z. Wang, Y. Bian, S. E. Shladover, G. Wu, S. E. Li, and M. J. Barth, "A survey on cooperative longitudinal motion control of multiple connected and automated vehicles," *IEEE Intelligent Transportation Systems Magazine*, 2019.

[17] E. Garone, S. Di Cairano, and I. Kolmanovsky, "Reference and command governors for systems with constraints: A survey on theory and applications," *Automatica*, vol. 75, pp. 306–328, 2017.

[18] A. Mesbah, "Stochastic model predictive control: An overview and perspectives for future research," *IEEE Control Systems Magazine*, vol. 36, no. 6, pp. 30–44, 2016.

[19] U. V. Kalabić, N. I. Li, C. Vermillion, and I. V. Kolmanovsky, "Reference governors for chance-constrained systems," *Automatica*, vol. 109, p. 108500, 2019.

[20] L. G. Khachiyan, "The problem of calculating the volume of a polyhedron is enumerably hard," *Russian Mathematical Surveys*, vol. 44, no. 3, p. 199, 1989.

[21] I. Kolmanovsky and E. G. Gilbert, "Theory and computation of disturbance invariant sets for discrete-time linear systems," *Mathematical problems in engineering*, vol. 4, no. 4, pp. 317–367, 1998.

[22] G. Orosz, "Connected cruise control: modelling, delay effects, and nonlinear behaviour," *Vehicle System Dynamics*, vol. 54, no. 8, pp. 1147–1176, 2016.